Available online at www.CivileJournal.org

Civil Engineering Journal

Vol. 5, No. 10, October, 2019

Mechanical Behavior of Hybrid Connectors for Rapid-Assembling Steel-Concrete Composite Beams

Senqiang Lu [a*], Wei Zhao [a], Puge Han [b], Zhenyuan Hang [a]

[a] *Road and Bridge department, Zhejiang institute of communications, Hangzhou 311112, China.*

[b] *Civil Engineering college, Jiangsu University of Science and Technology, Zhenjiang 212003, China.*

Received 23 June 2019; Accepted 28 August 2019

Abstract

In order to achieve a kind of shear connector suitable for rapid-assembling steel-concrete composite beams, a new type of hybrid shear connectors is proposed, in which the concrete slab with prefabricated circular holes and the steel beam with welded studs are installed and positioned, and then epoxy mortar is filled in the prefabricated hole to fix the studs. To study the mechanical behavior of these hybrid connectors, test on 18 push-out specimens with different prefabricated circular holes are carried out. ABAQUS finite element software is adopted to verify the relationship between the numerical simulation and experiment, influences of the epoxy mortar strength and prefabricated circular holes diameter are studied. The results show that filling epoxy mortar in the prefabricated hole is beneficial to improve the stiffness and bearing capacity of the specimen; the change of epoxy mortar strength has a certain impact on the bearing capacity and stiffness of the hybrid connector; In the case of the same strength of the filling material, the size of the prefabricated circular holes diameter directly affects the stiffness and bearing capacity of the shear stud. The shear capacity equations proposed by considering the epoxy mortar strength and prefabricated holes diameter, and it has a wide applicability.

Keywords: Rapid-Assembling; Hybrid Connectors; Strength of Epoxy Mortar; Prefabricated Circular Hole.

1. Introduction

Steel-concrete composite structures take advantages of using steel and concrete materials. It overcomes some limitations of material characteristics of sole material-based bridge structure performance, such as the low tensile strength of concrete and easy buckling of steel members under compression. The connection between steel and concrete significantly determines the overall performance of the composite structure. The treatment of the connect surface is the core in the design and construction of steel-concrete composite bridge.

Metallic connectors are traditionally used in steel-concrete composite bridge to connect the concrete slab and the steel beam. Shear connectors can resist the longitudinal shear force between concrete slabs and steel beams, and also resist the vertical lifting force between concrete slabs and steel beams [1-3].

Precast concrete deck system is very attractive for rapid replacement of the deteriorated concrete deck as well as new construction of composite bridges. Owing to the benefits of combining the two construction materials, it presents higher span-to-depth ratio, reduced deflections, and higher stiffness ratios than traditional steel or concrete beam structures. Because the precast deck system needs no framework in place and can save construction time, it can be applied especially

* Corresponding author: l7s7q@163.com

http://dx.doi.org/10.28991/cej-2019-03091395

to construction sites in the mountains, sea, and crowded cities. In the case of the replacement of a deteriorated concrete deck of a bridge located in a crowd city, this system can minimize the traffic interference.

For the rapid replacement of deteriorated concrete deck in steel-concrete composite bridges, the precast concrete deck system is very attractive and has been widely used. This system can be applied to the new construction of composite bridges, which has fewer steel girders and a wide spanning bridge deck.

The study of bonding steel beams to concrete slabs with building structural adhesive as shear connectors has shown the feasibility and practicability. However, due to the influence of adhesive materials, adhesive thickness, concrete strength, surface treatment methods, construction technology, the failure mode and mechanical behavior of bonded steel-concrete composite are not very clear. The first experiment on the bonded composite beams was carried out in 1962, Miklofsky et al. [4] compared a bonded composite beams with the mixed composite beams connected by the shear steel studs. These beams were prepared by directly depositing the fresh concrete on the epoxy adhesive, not hardened, on the steel beam surface. His testing results showed that the ruin of the mixed composite beam occurred by the crushing of the concrete, whereas the ruin of the bonded composite beams occurred due to the debonding failure of adhesive connection.

At the beginning of the 1970s, Hick and Baar [5] explored the bonded composite beams with surface treatment on the steel and concrete surfaces. For their system, the structural failure occurred due to shearing in the concrete slab near the adhesive joint. Hertig [6] also studied three different assembly processes. In the first system, the concrete was flowed on the steel girder surface, where aggregates were placed on the top of epoxy mortar. The second system consisted in bonding a prefabricated concrete slab with a steel girder by the help of fresh mortar. For the third system, the concrete was placed directly onto the fresh mortar which covered the steel surface. The results showed that the first system was most deformable; it enabled them to foresee the rupture of the composite beam by great deformations. The second system was the least resistant. The third system was most resistant but also most fragile.

Bouazaoui et al. [7] dealt with the experimental analysis of the mechanical behavior of bonded steel-concrete composite structures. The effect of the main parameters, such as the adhesive nature and the irregular thickness of the adhesive layer, on mechanical behavior and ultimate load was studied. The results showed that the connection between the steel girder and the concrete slab ensured by epoxy adhesive is perfect and without any slip in the steel–concrete interface.

According to the research status of composite beams, some progress has been made in the research of the two kinds of connectors. The related theories and calculation methods which can guide the engineering design and calculation have been also obtained. Nevertheless, there is no research on the shear connectors of the stud and epoxy mortar together, and the shear slip of the composite beams with hybrid connectors is obviously different from the conventional one. Therefore, the mechanical properties of the interface of hybrid connectors need to be further studied.

2. Experimental Program

2.1. Experimental Condition

In order to study the mechanical performance of the hybrid connectors, 4 groups of 18 specimens were designed and produced in accordance with the Eurocode 4 [8]. PT-C was the cast-in-situ specimen and PT-K was the specimen with hybrid connectors. The studs with diameter of 16 mm were consistently used for all specimens. Test results of the materials' properties are summarized in Table 1.

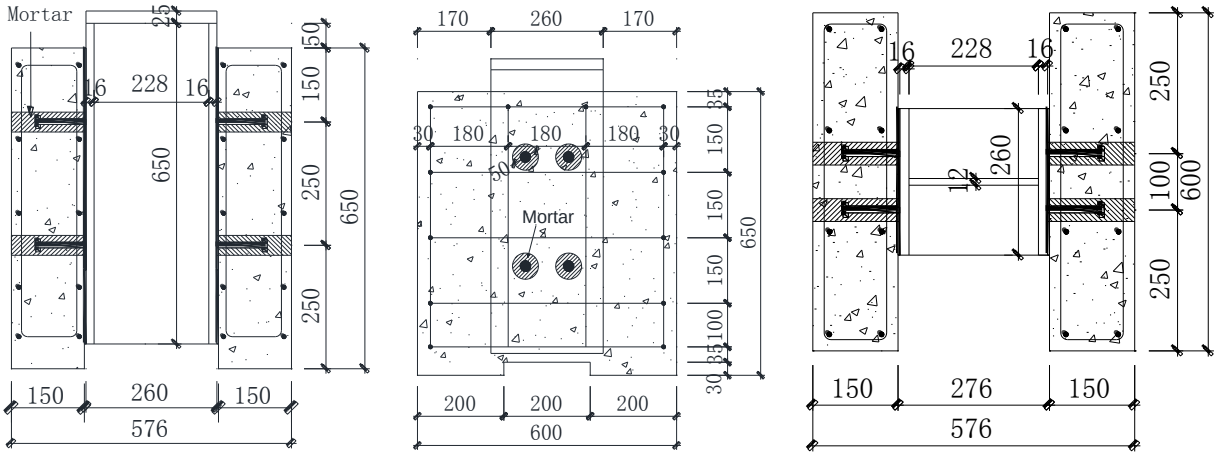

(a) Front view (b) Right view (c) Top view

Figure 1. Specimens' dimension (Unit: mm)

Table 1. Main parameters and material properties of the push-out test

Specimen group	Quantity	Prefabricated holes diameter (mm)	Elastic modulus of epoxy mortar (MPa)	Epoxy mortar		Stud strength		Compressive strength of concrete (MPa)
				Compressive strength (MPa)	Tensile strength (MPa)	f_y (MPa)	f_{std} (MPa)	
PT-K40	5	40						
PT-K50	5	50	12289.03	109.73	25.51	279	450	39.2
PT-K60	5	60						
PT-C	3	-	-	-	-			

2.2. Experimental Method

The test adopted the jack continuous loading mode and applies pressure on the top of the specimen. Sand was placed on the top of testing specimen to ensure that no eccentricity occurred during the loading process. In the early stage, 30 kN loading level was adopted. When the loading curve appears an obvious inflection point, 20 kN loading level was adopted. Before and after each loading stage, the slip data was read once.

3. Experimental Results

3.1. Failure Mode

At the early stage of loading, there was no obvious test phenomenon, except for the change of dial reading. Group PT-K specimens were characterized by structural unilateral separation and the failure modes of specimens mainly came from the stud shear failures (Figure 2a). The epoxy mortar in the root of the stud was crushed locally, as shown in Figure 2(b). The concrete appeared to be locally crushed in the Group PT-C specimens, as shown in Figure 2(c). Some Group PT-K40 and Group PT-K50 specimens presented some cracks in the concrete around the holes, only Group PT-K60 specimens did not show this phenomenon.

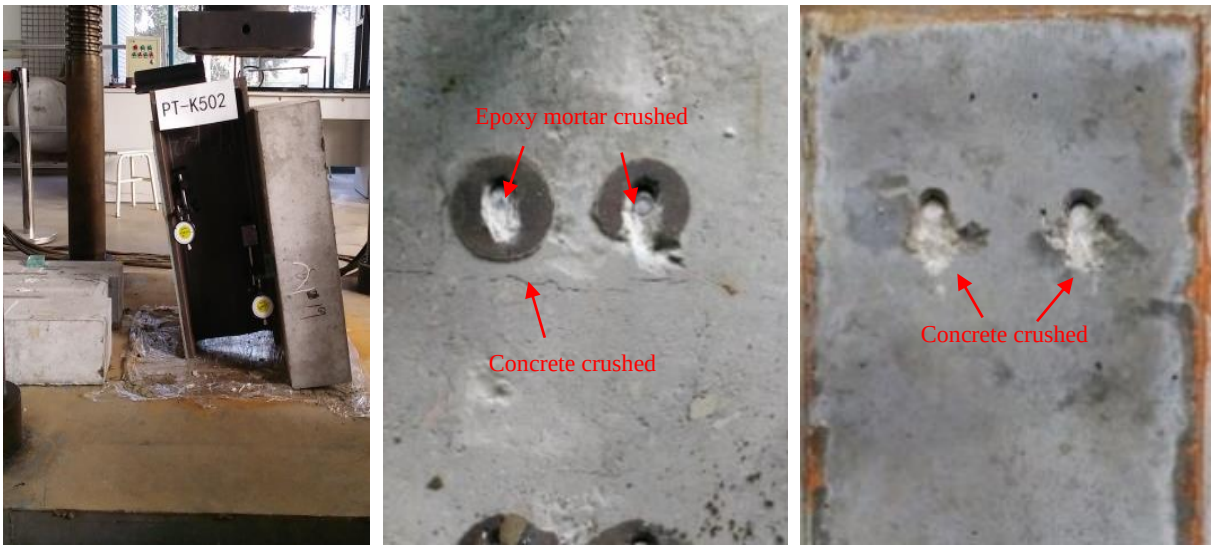

(a) (b) (c)

Figure 2. Failure patterns of representative specimens after push-out test

3.2. Bearing Capacity and Slip Performance

The load-slip curve is one of the important indexes to study the behavior of shear keys. The slip between the steel beam and the concrete slab during the loading process was measured by the dial gauge. The mechanical behaviors of Group PT-K specimens during the completed loading process were analyzed according to the load-slip curves (see Figure. 3). The differences of mechanical properties between Group PT-K and PT-C were investigated as well. In this test, the deviation values of each group are less than 10%, and the specimen with the lowest limit load in each group is selected to compare. The cracking load, the ultimate load and the corresponding slip values are extracted from the experimental data and the stiffness calculation method of the shear connectors in Eurocode 4 is adopted. The calculated results are given in Table 2.

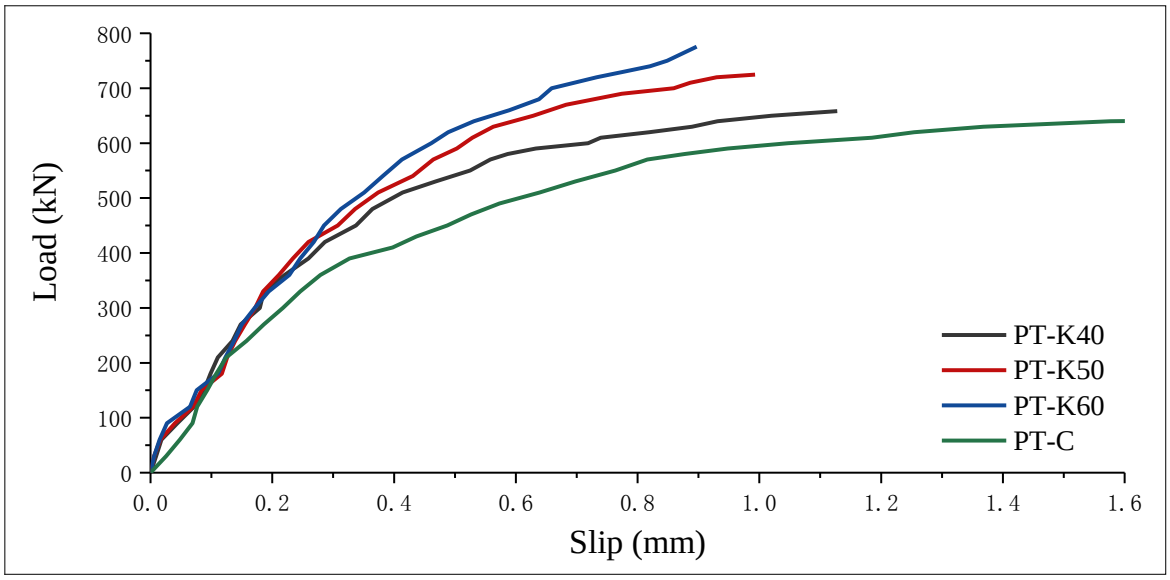

Figure 3. Load versus slip at stud position curve

Table 2. Test result

Specimen group	dh/dstd	Cracking load Pk/kN	Cracking load corresponding slip /mm	Ultimate load Pu/kN	Ultimate load corresponding displacement /mm
PT-K40	2.5	450	0.338	658.24	1.128
PT-K50	3.125	510	0.374	724.68	0.993
PT-K60	3.75	590	0.461	775.58	0.897
PT-C	/	270	0.186	643.31	1.860

As shown in Figure 3, before the load reaches 200 kN, the load slip curve of the specimen is approximately linearly increased with the load. The relative slip between the steel beam and concrete plate is less than 0.1mm. When the load slip curve begins to enter the nonlinearity, the load is up to 260 kN. The minimum cracking load value (450 kN) of the three PT-K specimens is higher than that of PT-C specimen (270 kN), which indicates that the epoxy mortar can prevent the crack under low stress due to its higher tensile strength. The ultimate load of PT-K specimen is greater than that of PT-C, and the relative slip decreases significantly, indicating that the ultimate bearing capacity and relative slip can be effectively improved by the epoxy mortar. In addition, the bearing capacity and stiffness of three PT-K specimens were revealed as PT-K60 > PT-K50 > PT-K40. It is implied that the size of the prefabricated holes diameter also remarkably affect the bearing capacity and stiffness of specimen under the same material strength.

4. Finite Element Analysis

In this study, the commercial finite elements (FE) software ABAQUS was used to simulate the push-out test. To obtain more accurate results from the FE analysis, all components influencing the behavior of the shear connector were properly modeled. Both geometric and material nonlinearities were taken into consideration in the FE analysis.

4.1. Finite Element Mesh

Considering the symmetry of the specimens, only one quarter of the push out test arrangement was modeled. For concrete slabs, steel beam, epoxy mortar and studs, a 3D eight-node element (C3D8R) was used, which also improved the rate of convergence. A two-node linear 3D truss element (T3D2) was adopted for the steel reinforcement. To improve the accuracy of the calculation, a fine mesh was adopted for the studs and epoxy mortar. The approximate overall mesh scale was 20 mm, with the smallest mesh scale being about 5 mm. The FE mesh of the push out test model is depicted in Figure 4.

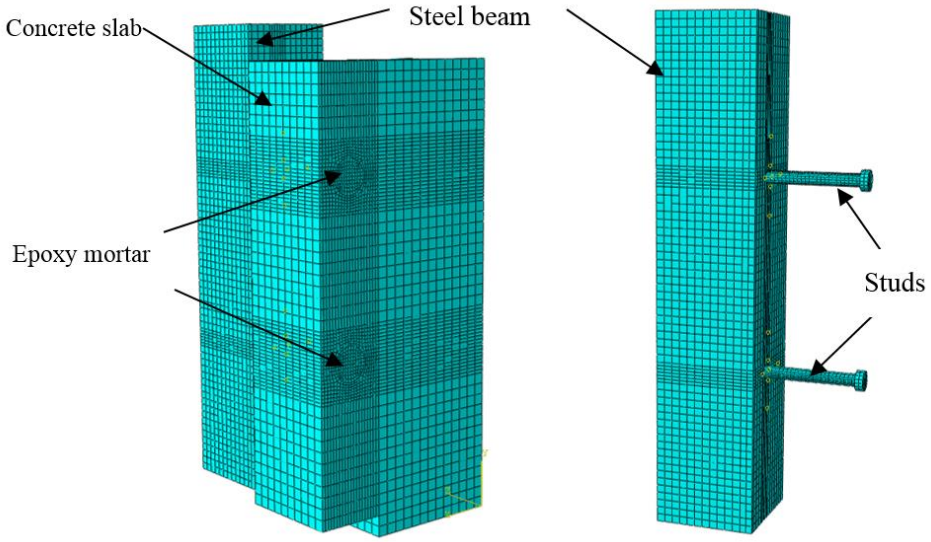

Figure 4. Finite element mesh of model

4.1.1. Material Constitutive Model

The compressive stress-strain curves of concrete with different strength grades proposed in the previous study [7] were used in finite element models, and the equation is as follows.

$$y=\begin{cases}\dfrac{A_1x+(B_1-1)x^2}{1+(A_1-2)x+B_1x^2} & (x\le 1)\\ \dfrac{x}{\alpha_1(x-1)^2+x} & (x>1)\end{cases} \tag{1}$$

In the Equation 1, $y=\sigma/f_c$, σ is stress, f_c is the axial compressive strength of concrete, $f_c=0.4f_{cu}^{7/6}$, f_{cu} is cubic compressive strength of concrete, $x=\varepsilon/\varepsilon_c$, ε is compressive strain of concrete, and ε_c is compressive peak strain of concrete. $\varepsilon_c=383f_{cu}^{7/18}\times10^{-6}$, A_1 is the ratio of the elastic modulus to the peak secant modulus of concrete, $A_1=9.1f_{cu}^{-4/9}$ and B_1 is the physical quantity to control the attenuation of the elastic modulus of the ascending portion, $B_1=1.6(A_1-1)^2$, α_1 is the parameter of the descending portion of the stress-strain curve of the concrete uniaxial compression. Because the concrete is in the state of local pressure, $\alpha_1=0.15$ is taken.

The constitutive model of epoxy mortar is not clear, the constitutive model adopted in this paper is modified on the basis of Equation 1, which considering the properties of the material are similar to that of concrete. f_c is replaced by the compressive strength value f_h of epoxy mortar and f_{hu} is used to replace the cubic compressive strength of concrete, other parameters also change accordingly.

The linear reinforcement elastoplastic model is adopted for the steel beam, studs and reinforcing bars. Von Mises yield criterion is adopted in the material constitutive equation. In the test, it was found that the PT-K specimens were all marked by the failure of the studs at the end of the test. Therefore, the stud is characterized by three-phase linear model, and the stress-strain relation is expressed by Equation 2. The steel beam and the bars used the ideal elastoplastic model, the equation of stress-strain relationship can be seen in Equation 3.

$$\sigma_i=\begin{cases}E_s\varepsilon_i & (\varepsilon_i\le\varepsilon_y)\\ f_y+0.01E_s(\varepsilon_i-\varepsilon_y) & (\varepsilon_y<\varepsilon_i\le\varepsilon_u)\\ f_{std}=1.2f_y & (\varepsilon_i>\varepsilon_u)\end{cases} \tag{2}$$

$$\sigma_i=\begin{cases}E_s\varepsilon_i & (\varepsilon_i\le\varepsilon_y)\\ f_y & (\varepsilon_i>\varepsilon_y)\end{cases} \tag{3}$$

In Equations 2 and 3, σ_i is the equivalent stress of steel, f_y is the yield strength of steel, f_{std} is the yield strength of steel, E_s is the elastic modulus of steel, ε_i is the equivalent strain of steel, ε_y is the strain of steel yield, and ε_u is the strain when the steel reaches the ultimate strength.

4.1.2. Interface Treatment

The contact between the epoxy mortar and the concrete plate consisted of two parts, namely the normal and tangential penalty function. The contact between the steel beam and the concrete plate was 'Frictionless surface to surface contact', the bonding between the steel beam and the concrete was not taken into account. The studs and reinforcing bars were embedded in epoxy mortar and concrete slab respectively, ignoring the bond slip between the stud and epoxy mortar. The effects of the relative slip and separation of the epoxy mortar with respect to the concrete slabs were ignored.

4.2. Finite Element Model Verification

The load-slip curves obtained by the finite element simulation are compared with the test curves and is shown in Figure 5. The ultimate bearing capacity and the initial stiffness of the finite element analysis match well with the test (Table 3). The mean value of the experiment over finite element load is 1.03, it shows that both of them are within acceptable agreement, which indicates that the nonlinear finite element method can simulate the load-slip relationship of the stud specimen, and it is suitable for further parametric study.

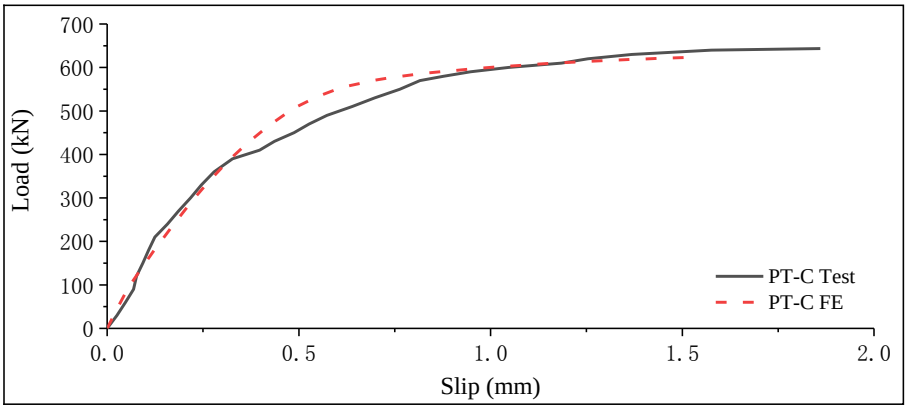

(a)

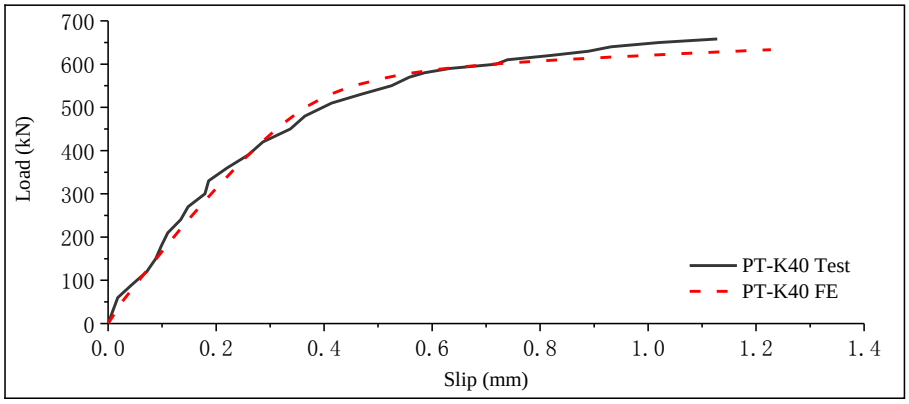

(b)

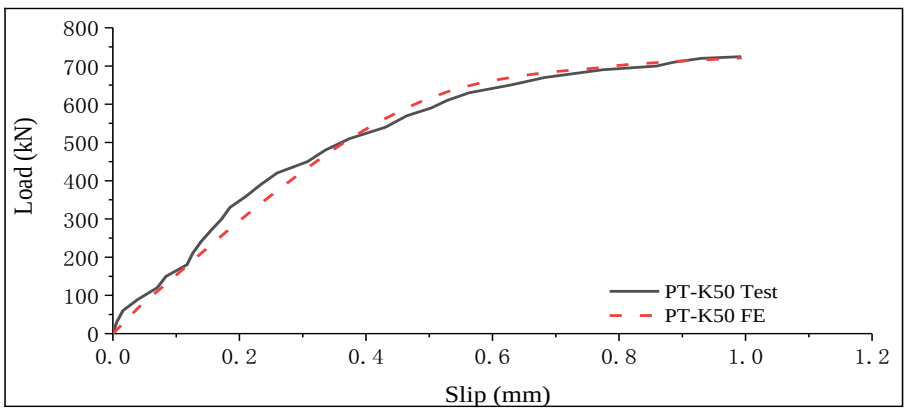

(c)

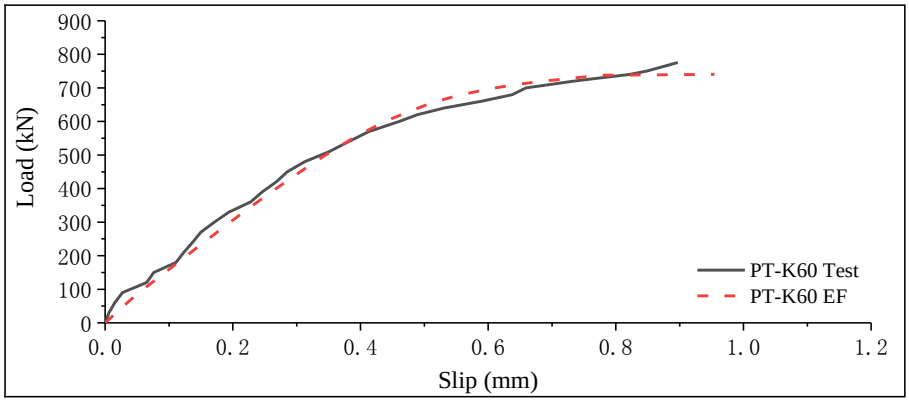

(d)

Figure 5. Comparison of experiment and FE load-slip curves

Table 3. Comparison of shear connector strength from push tests and finite element analysis

Specimen group	Experimental load, P_{test} (kN)	Load from FE, P_{FEA} (kN)	P_{test} / P_{FEA}
PT-K40	658.24	633.21	1.04
PT-K50	724.68	721.12	1.00
PT-K60	775.58	740.28	1.05
PT-C	643.31	622.77	1.03
Mean			1.03

Stress contours of a typical PT-K component are given in Figure 6, the stress of the steel beam is small when the PT-K specimen is destroyed. The stress in the stud is reduced from the root to the top gradually, and the root of the stud is first entered into the plastic, the compression side of the epoxy mortar at the root of the stud is partially crushed. The concrete has no local crushing, which coincides well with the experimental phenomenon (Figure 2b).

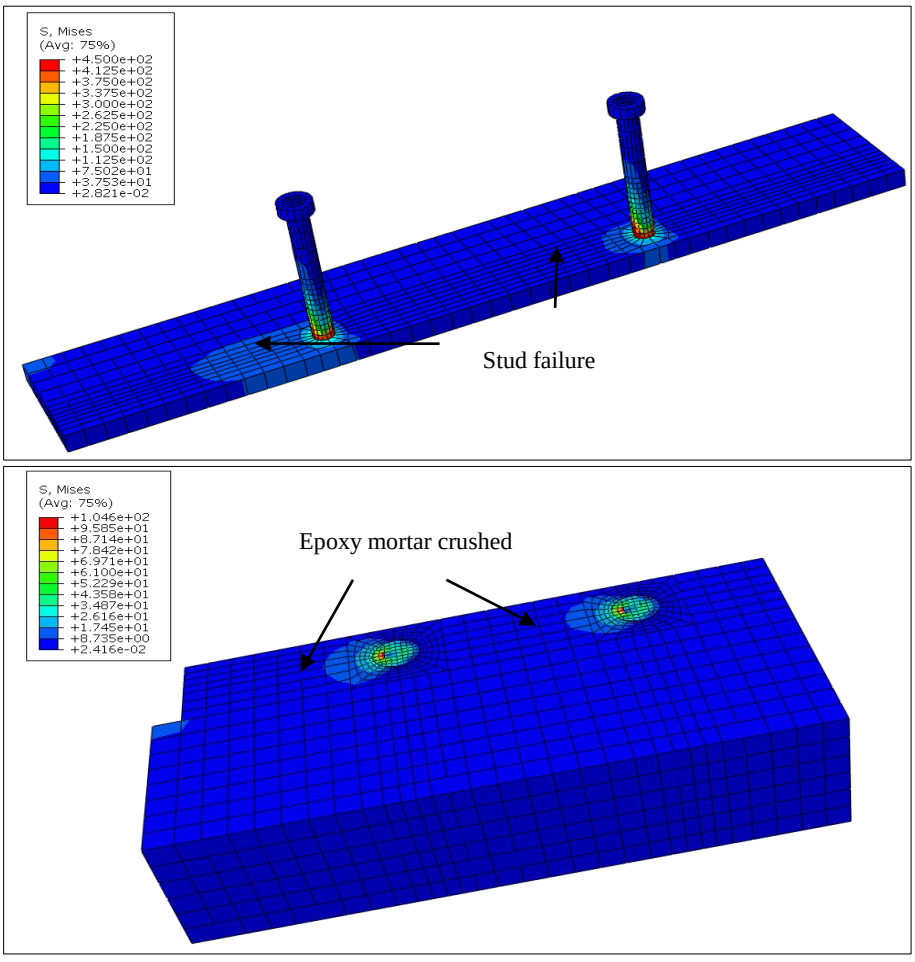

Figure 6. Stress contours from FE model for specimen PT-K50 (a) Stud failure; (b) Epoxy mortar crushed

4.3. Parametric Study

In order to study the influence of more parameters on the bearing capacity, stiffness and relative slip of the hybrid shear connectors, the 3.1 section finite element method was used. 8 kinds of epoxy mortar with different strengths were calculated by 3D finite element method.

4.3.1. Load-slippage Curves

The shear connector model with prefabricated circular hole diameter of 50 mm was taken as an example, while the strength values of epoxy mortar (50, 60, 70, 80, 90,100, 110 MPa and 120 MPa) were taken as the change parameters. The load-slip curves of the different strength of epoxy mortar can be found in Figure 7. The ultimate load, the slip corresponding to the ultimate load and the stiffness of a single stud are given in Table 4. It is seen that the initial stiffness and bearing capacity of the PT-C specimens are obviously lower than those of the PT-K specimens. The higher the strength of epoxy mortar, the higher the bearing capacity and stiffness of the specimen. But the relationship between them is nonlinear, when the strength of the mortar is greater than 80 MPa, the growth trend is not obvious.

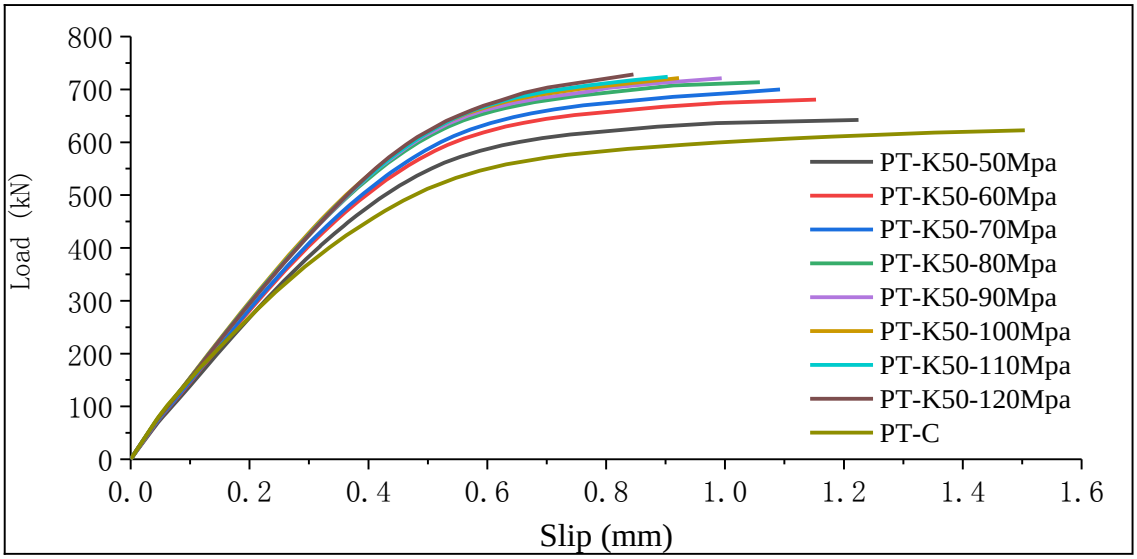

Figure 7. Effect of strength of the epoxy mortar

Table 4. Finite element simulation results

Specimen	f_{hu} / f_{std}	Ultimate load Pu/kN	Recruitment compared with PT-C (%)	Ultimate load corresponding displacement (mm)	Recruitment compared with PT-C (%)
PT-K50-50Mpa	0.111	642.11	3.11	1.225	18.60
PT-K50-60Mpa	0.133	680.64	9.29	1.153	23.39
PT-K50-70Mpa	0.156	699.90	12.38	1.093	27.38
PT-K50-80Mpa	0.178	713.33	14.54	1.059	29.63
PT-K50-90Mpa	0.2	721.12	15.79	0.995	33.89
PT-K50-100Mpa	0.222	721.70	15.89	0.923	38.67
PT-K50-110Mpa	0.244	724.00	16.25	0.903	40.00
PT-K50-120Mpa	0.267	728.36	16.95	0.846	43.78
PT-C	-	622.77	-	1.505	-

4.3.2 .Stress Distribution Curve

The axial stress and shear stress data along the stud axial direction under 40 kN external force are extracted from the finite element calculation results, to study the effect of prefabricated holes size and strength of epoxy mortar on the stud stress, as shown in Figures 8 and 9.

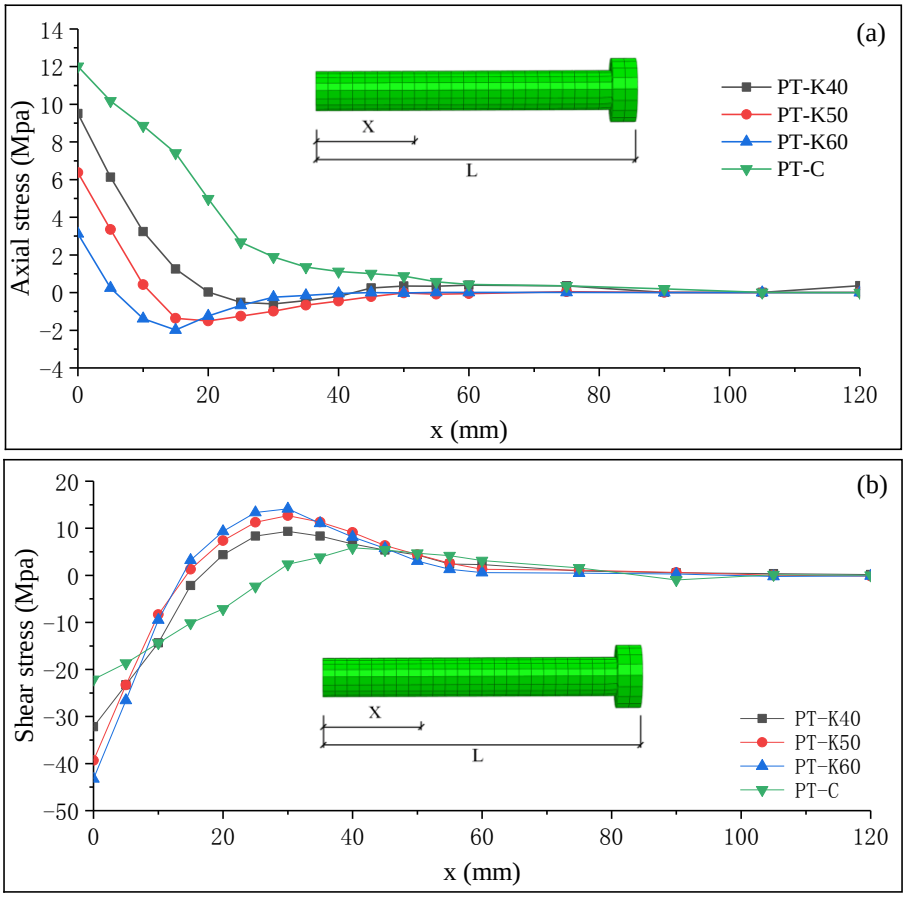

Figure 8. Longitudinal distribution of stress in stud section center (a) Axial stress (b) Shear stress

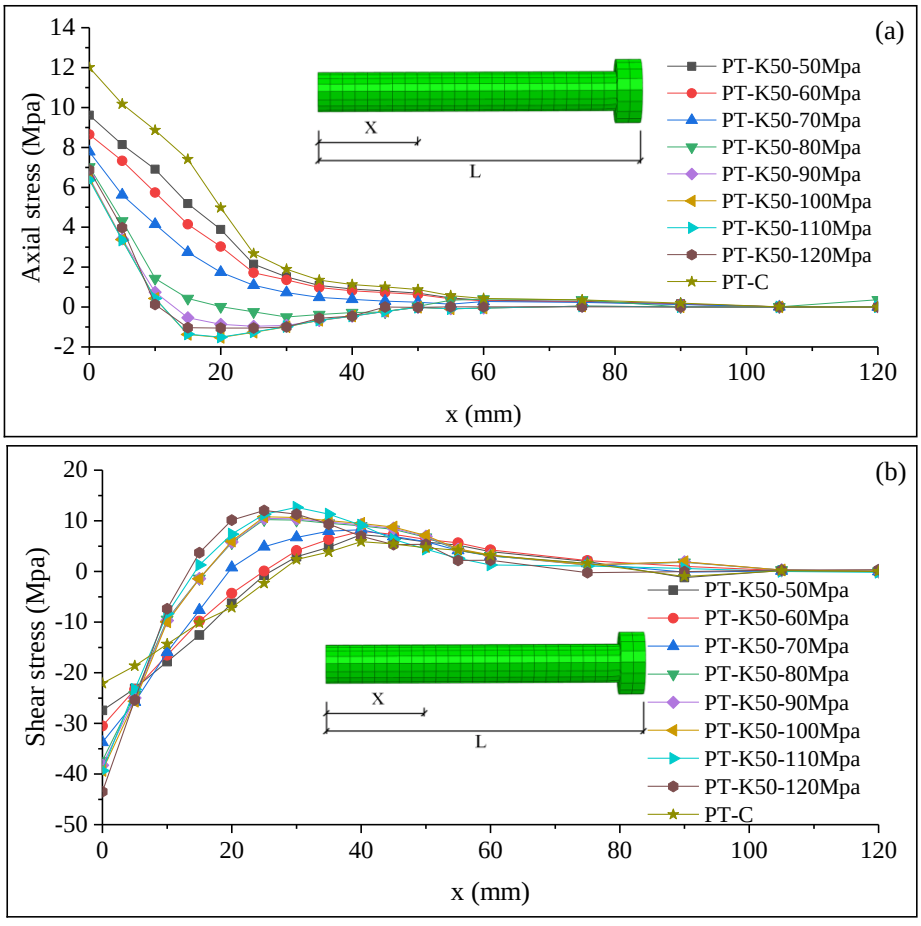

Figure 9. Longitudinal distribution of stress in stud section center (a) Axial stress (b) Shear stress

The axial and shear stresses of stud are mainly concentrated in the lower part of 1/3. The axial stress of PT-C specimens is obviously greater than that of PT-K specimens at the root of the stud, while the shear stress is obviously smaller than that of PT-K specimens, so the ratio of shear stress to axial stress of the root of PT-C studs is larger than that of PT-K. This indicates that epoxy mortar with high strength can increase the bending stiffness of the whole connector, which reduces the corresponding bending deformation, thus the shear deformation is dominant. For the PT-K specimens with different prefabricated holes diameter, the shear stress at the nail root of PT-K60 specimens is higher than that of the other two specimens, but the tensile stress at the root of PT-K60 specimens is obviously smaller than that of the other two specimens. It indicates that the stud has greater bending stiffness with the increase of the prefabricated holes diameter, and the bending stress is smaller at the initial loading stage. Correspondingly, for the PT-K specimens with different epoxy mortar strength, the axial stress at the stud root of the 8 PT-K specimens decreases slowly with the increase of the strength of epoxy mortar, and the shear stress increases slightly.

5. Theoretical Analysis

5.1. Force Transfer Mechanism

Combined with the stress contours obtained in ABAQUS (Figures 10 and 11), the concentrated force P caused by a single stud can be decomposed horizontally and vertically. The transverse component P_L is mainly caused by the bending deformation of the stud, which leads to the separation of the concrete slab and the steel beam; the vertical component P_V is the shear force caused by the slip between the concrete slab and the steel beam, which produces the diffusive angle during the transfer of the concrete slab and the transverse tensile force T_{split}, causes the cracking of the concrete slab in front of the stud. A strut and tie model can be established to reflect its stress mechanism, See Figure 12(b). The distribution of transverse tension in vertical direction of PT-C specimen is shown in Figure 12(c), for the PT-K specimens, the crack development is delayed because the epoxy mortar is in a large transverse tensile position. In addition, the bending deformation of stud is hard to occur due to the influence of epoxy mortar, and the slip between steel plate and concrete is significantly reduced.

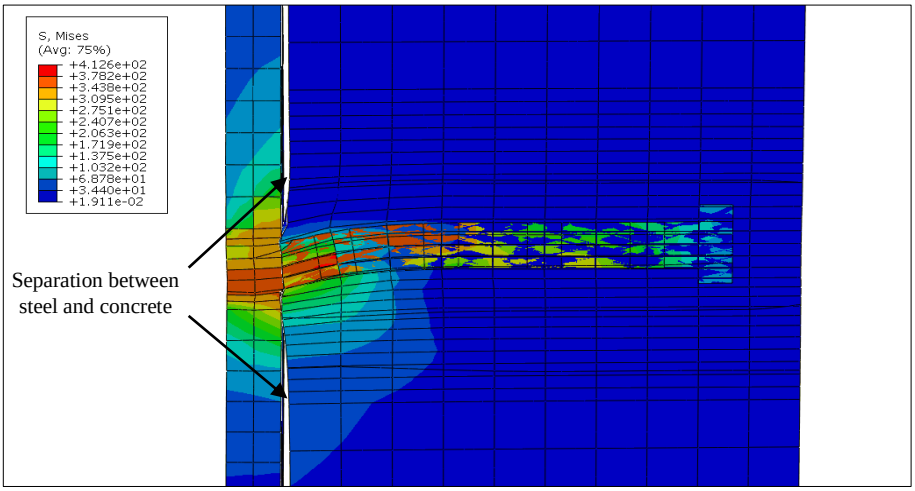

Figure 10. Deformation of stud at a certain stage

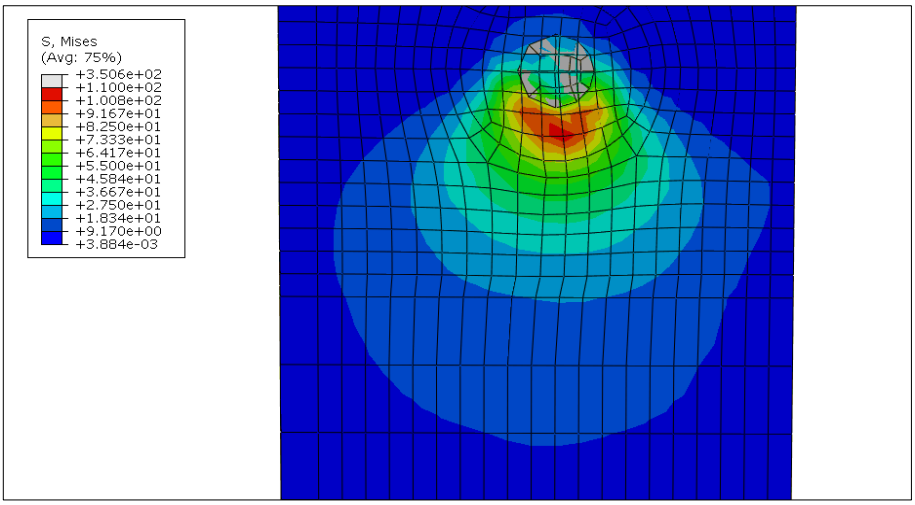

Figure 11. Stress distribution of stud root

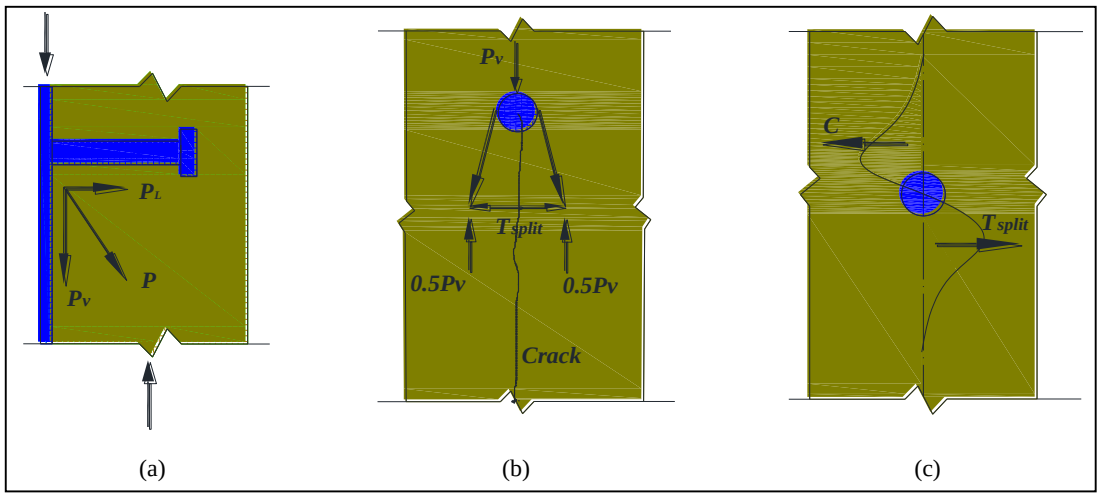

Figure 12. Force transmission mechanism

5.2. Calculation Equation

According to the test and the finite element calculation results, the shear failure of four studs on one side occurs simultaneously when the specimen reaches the ultimate bearing capacity, which indicates that the shear bonds basically reach the ultimate bearing capacity under the ultimate load state. Therefore, it can be concluded that the shear capacity of specimens with 4 shear connectors is 4 times of that with a single shear connector. According to the test and finite element analysis, the bearing capacity of a single hybrid connector is affected by the epoxy mortar and prefabricated holes size. From Eurcode 4, the equation of the shear bearing capacity of a single stud is also affected by the material strength and elastic modulus of the stud. Therefore, the shear bearing capacity of a single hybrid connector presented in this paper can be calculated from the following Equation 4 [9-15]:

$$N_v^c = A_{std} f_{std} \left(\frac{E_h}{E_s}\right)^{0.2} \left(\frac{f_{hu}}{f_{std}}\right)^{0.1} \left(\frac{d_h}{d_{std}}\right)^{0.6} \quad (4)$$

In Equation 4, A_{std} is the cross-section area of the stud, f_{std} is the tensile strength of the stud, the E_h is the elastic modulus of concrete, the E_s is the elastic modulus of the stud, the f_{ch} is the compressive strength of concrete, the d_h is the diameter of prefabricated hole, and the d_{std} is the diameter of the stud. The bearing capacity of a single shear bond calculated by Equation 4 is compared with test results and finite element results (See Table 3).

Table 5. Comparison between theoretical formula and experiment and FE

Specimen number	Fitting equation (kN)	Push-out test (kN)	Deviation of fitting equation and experimental value (%)	Finite element calculation (kN)	Deviation of fitting equation and finite element calculation (%)
PT-K40	619.93	658.24	5.8	-	-
PT-K50	708.74	724.68	2.18	-	-
PT-K60	790.67	775.58	1.96	-	-
PT-K50-50Mpa	655.01	-	-	642.11	2.00
PT-K50-60Mpa	667.06	-	-	680.64	1.94
PT-K50-70Mpa	677.42	-	-	699.90	3.21
PT-K50-80Mpa	686.53	-	-	713.33	3.76
PT-K50-90Mpa	694.67	-	-	721.12	3.67
PT-K50-100Mpa	702.02	-	-	721.70	2.73
PT-K50-110Mpa	708.75	-	-	724.00	2.11
PT-K50-120Mpa	714.94	-	-	728.36	1.84

The maximum deviation between Equation 4 and test results and finite element analysis results is about 5.8%, which is acceptable and can be selected for calculating the shear capacity of this kind of shear connectors. However, regarding the safety of the project, the safety factor should be introduced according to the actual demand.

6. Conclusions

Through the experimental study and finite element parameter analysis of the new type connection of the rapid assembled steel-concrete composite beam, the following conclusions and suggestions are obtained:

- Filling epoxy mortar in the stud hole is beneficial to improve the stiffness and shear bearing capacity of the specimen; the change of epoxy mortar strength has a certain impact on the bearing capacity and stiffness of the hybrid connector; In the case of the same strength of the filling material, the size of the stud hole diameter directly affects the stiffness and bearing capacity of the shear stud.
- The proposed equation is acceptable in terms of shear capacity and experimental and finite element results and can be applied to practical engineering.
- There is no study on different grades and height of stud, so it is necessary to carry out the experimental study on these parameters in the future.

7. Funding

This work was supported by Science and Technology Project of Zhejiang Provincial Communication Department (Code number of project: 2018004).

8. Conflicts of Interest

The authors declare no conflict of interest.

9. References

[1] Chapman JC. "Composite construction in steel and concrete. The behavior of composite beams." The Structural Engineering (1964); 42.

[2] Barnard, P R, and R P Johnson. "Ultimate Strength of Composite Beams." Proceedings of the Institution of Civil Engineers 32, no. 2 (October 1965): 161–179. doi:10.1680/iicep.1965.9226.

[3] Trouillet P. "Comportement local de connecteurs acier/beton sollicites au cisaillement-etude bibliographique." Rapports des laboratoires. Serie:Ouvrages d'art OA-3; (1987).

[4] Miklofsky HA, Brpown MR, and Gonsior MJ. "Epoxy bending compounds as shear connectors in composite beams. "State of New York: Dept. of Public Works, Eng. Res Series. RR.62-2; (1962).

[5] Hick F, and Baar S. "Structures metalliquescollees. Station d'Essaiset de Recherches de la Construction Metallique." SERCOM.Belgique; (1972).

[6] Hertig PH, and Perret A. "Rapport d'Essais de trois types de liaisons acierbetonal'aide de mortiersepoxys."Ecole Polytechnique Federalede Lausanne, Institut de la Construction Metallique; (1973).

[7] Bouazaoui, L., G. Perrenot, Y. Delmas, and A. Li. "Experimental Study of Bonded Steel Concrete Composite Structures." Journal of Constructional Steel Research 63, no. 9 (September 2007): 1268–1278. doi:10.1016/j.jcsr.2006.11.002.

[8] Eurcode 4-"Design of composite steel and concrete structures-Part 2: General rules and rules for bridges." Brussels, Belgium: European Committee for Standardization, (2005).

[9] Ollgaard J.G, SlutterR.G, and Fisher J.W. "Shear strength of stud connectors in lightweight and normal-weight concrete." AISC Engineering Journal.,(1971),8 (2) :55-64.

[10] NieJianguo. "Test theory and application of steel-concrete composite beams." Beijing: Science Press, (2005): 298-316.

[11] Ding, Faxing, Xiaoyong Ying, Linchao Zhou, and Zhiwu Yu. "Unified Calculation Method and Its Application in Determining the Uniaxial Mechanical Properties of Concrete." Frontiers of Architecture and Civil Engineering in China 5, no. 3 (September 2011): 381–393. doi:10.1007/s11709-011-0118-6.

[12] Badie, Sameh S., Amgad F. Morgan Girgis, Maher K. Tadros, and Nghi T. Nguyen. "Relaxing the Stud Spacing Limit for Full-Depth Precast Concrete Deck Panels Supported on Steel Girders (Phase I)." Journal of Bridge Engineering 15, no. 5 (September 2010): 482–492. doi:10.1061/(asce)be.1943-5592.0000082.

[13] Berthet, J.F., I. Yurtdas, Y. Delmas, and A. Li. "Evaluation of the Adhesion Resistance between Steel and Concrete by Push out Test." International Journal of Adhesion and Adhesives 31, no. 2 (March 2011): 75–83. doi:10.1016/j.ijadhadh.2010.11.004.

[14] Nguyen, Huu Thanh, and SeungEock Kim. "Finite Element Modeling of Push-Out Tests for Large Stud Shear Connectors." Journal of Constructional Steel Research 65, no. 10–11 (October 2009): 1909–1920. doi:10.1016/j.jcsr.2009.06.010.

[15] ANSI /AISC 360-05"Specification for structural steel buildings."Chicago,IL: American Institute of Steel Construction, (2005).